Osheroff, N. (1989a) *Pharmacol. Ther. 41*, 223-241.
Osheroff, N. (1989b) *Biochemistry 28*, 6157-6160.
Osheroff, N., & Zechiedrich, E. L. (1987) *Biochemistry 26*, 4303-4309.
Osheroff, N., Shelton, E. R., & Brutlag, D. L. (1983) *J. Biol. Chem. 258*, 9530-9535.
Pommier, Y., Minford, J. K., Schwartz, R. E., Zwelling, L. A., & Kohn, K. W. (1985) *Biochemistry 24*, 6410-6416.
Robinson, M. J., & Osheroff, N. (1990) *Biochemistry 29*, 2511-2515.
Sander, M., & Hsieh, T.-S. (1983) *J. Biol. Chem. 258*, 8421-8428.
Sander, M., Hsieh, T.-S., Udvardy, A., & Schedl, P. (1987) *J. Mol. Biol. 194*, 219-229.
Shelton, E. R., Osheroff, N., & Brutlag, D. L. (1983) *J. Biol. Chem. 258*, 9530-9535.
Tewey, K. M., Chen, G. L., Nelson, E. M., & Liu, L. F. (1984) *J. Biol. Chem. 259*, 9182-9187.
Uemura, T., & Yanagida, M. (1984) *EMBO J. 3*, 1737-1744.
Uemura, T., & Yanagida, M. (1986) *EMBO J. 5*, 1003-1010.
Uemura, T., Ohkura, H., Adachi, Y., Morino, K., Shiozaki, K., & Yanagida, M. (1987) *Cell 50*, 917-925.
van Maanen, J. M. S., Retel, J., de Vries, J., & Pinedo, H. M. (1988) *J. Natl. Cancer Inst. 80*, 1526-1533.
Vosberg, H.-P. (1985) *Curr. Top. Microbiol. Immunol. 114*, 19-102.
Wang, J. C. (1985) *Annu. Rev. Biochem. 54*, 665-697.
Yang, L., Rowe, T. C., & Liu, L. F. (1985) *Cancer Res. 45*, 5872-5876.
Zechiedrich, E. L., Christiansen, K., Andersen, A. H., Westergaard, O., & Osheroff, N. (1989) *Biochemistry 28*, 6229-6236.
Zwelling, L. A. (1985) *Cancer Metastasis Rev. 4*, 263-276.
Zwelling, L. A., Hinds, M., Chan, D., Mayes, J., Sie, K. L., Parker, E., Silberman, L., Radcliffe, A., Beran, M., & Blick, M. (1989) *J. Biol. Chem. 264*, 16411-16420.

Kinetic and Equilibrium Analysis of a Threading Intercalation Mode: DNA Sequence and Ion Effects†

Farial A. Tanious, Shau-Fong Yen,‡ and W. David Wilson*
Department of Chemistry and Laboratory for Chemical and Biological Sciences, Georgia State University, Atlanta, Georgia 30303

Received September 6, 1990; Revised Manuscript Received November 19, 1990

ABSTRACT: The interaction of a symmetric naphthalene diimide with alkylamino substituents at each imide position was investigated with the alternating sequence polymers, poly[d(A-T)]$_2$ and poly[d(G-C)]$_2$. Spectrophotometric binding studies indicate strong binding of the diimide to both sequences although the GC binding constant is 20-25 times larger than the AT binding constant. Analysis of the effects of salt concentration on the binding equilibria shows that the diimide forms two ion pairs in its complex with both polymers as expected for a simple dication. Stopped-flow kinetics experiments demonstrate that the diimide both associates and dissociates from DNA more slowly than classical intercalators with similar binding constants. Analysis of salt concentration effects on dissociation kinetics rate constants (k_d) reveals that slopes in log k_d versus log [Na^+] plots are only approximately half the value obtained for classical dicationic intercalators that have both charged groups in the same groove. These kinetics results support a threading intercalation model, with one charged diimide substituent in each of the DNA grooves rather than with both side chains in the same groove, for the diimide complex with DNA. In the rate-determining step of the mechanism for dissociation of a threading complex only one ion pair is broken; the free side chain can then slide between base pairs to put both diimide side chains in the same groove, and this is followed by rapid full dissociation of the diimide. This sequential release of ion pairs makes the dissociation slope for dicationic threading intercalators more similar to the slope for classical monocationic intercalating ligands. Kinetics studies, thus, provide a very clear method for distinguishing classical from threading intercalators. Similar experiments can also distinguish intercalation from groove binding modes.

Simple intercalators, such as proflavin, bind to DNA with essentially all of their aromatic system (e.g., their entire molecular structure) inserted between the base pairs that form the top and bottom of the intercalation site (Waring, 1981; Neidle & Abraham, 1984; Wilson, 1990). Most natural and synthetic intercalators, however, have substituents of varying chemical nature, steric bulk, and charge which lie in one of the DNA grooves after insertion of the planar aromatic system of the intercalator between base pairs. Detailed crystallographic and NMR studies have shown that many well-characterized intercalators such as ethidium (Jain et al., 1977; Tsai et al., 1977), actinomycin (Sobell & Jain, 1972; Scott et al., 1988), and daunomycin (Wang et al., 1987) intercalate with DNA such that their bulky substituents are in the minor groove. Lower resolution experiments (binding, hydrodynamic, etc.) coupled with modeling studies have suggested that many acridine intercalators, such as the anticancer drug amsacrine, also bind with their bulky substituents in the minor groove (Denny et al., 1983; Abraham et al., 1988).

Several recently characterized intercalators, however, form DNA complexes with bulky and/or charged substituents in the major groove of the double helix. A group of unfused aromatic intercalators, which are amplifiers of the bleomycin-catalyzed cleavage of DNA, bind to DNA in such a major groove complex (Wilson et al., 1988, 1989b). Some aromatic

† This work was supported by Grant NIH-NIAID AI-27196.
‡ Present address: Ciba Vision Corp., Atlanta, GA 30360.

0006-2960/91/0430-1813$02.50/0

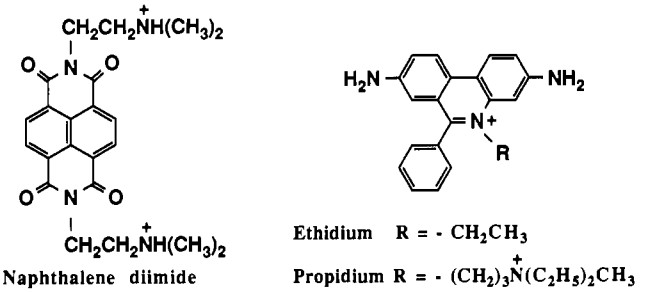

FIGURE 1: Structures of the naphthalene diimide, ethidium, and propidium.

diamidines, such as DAPI, which bind in the minor groove at AT sequences, intercalate at GC or mixed sequences and have their diamidine groups in the major groove (Wilson et al., 1989a, 1990a–c). Detailed NMR studies have shown that the acridine bisintercalator, ditercalinium, binds to DNA with both acridine rings intercalated and with the linking chain in the major groove (Delbarre et al., 1987).

The insertion of a simple aromatic ring system such as anthracene between DNA base pairs to form an intercalation complex requires separation of adjacent base pairs by 3.4 Å in the thermally induced molecular dynamics of the double helix (Waring, 1981; Neidle & Abraham, 1984; Wilson, 1990). Addition of a simple cationic side chain at the 9-position of anthracene should not significantly change the complex or the mechanism of binding since the chain would be in one of the DNA grooves and the complex would have the long axis of the anthracene ring stacked over the base pairs at the intercalation site. If side chains are added to both the 9- and 10-positions, on opposite sides of the anthracene ring, however, one substituent must slide between base pairs during formation of the intercalation complex, and this should decrease the rates for the binding reaction.

We designed a series of naphthalene diimide intercalators, with charged side chains of varying size on opposite sides of the intercalating ring system (example structure in Figure 1), to determine whether such compounds can bind to DNA by intercalation if the binding mechanism requires sliding of one of the charged groups through the helix (Yen et al., 1982). Clearly, as the substituents on opposite sides of the intercalator increase in size, larger and larger openings in the double helix would be required to allow insertion of the aromatic ring system. After the bulky substituent has passed through the double helix, however, the base pairs on adjacent sides of the intercalation site can assume a normal intercalation geometry and can stack on the aromatic system of the intercalator. This threading binding mechanism, which requires significant distortion of the double helix in intermediate states but which produces a fairly standard final intercalation complex, has energetics of complex formation that are in the range generally expected for intercalation but has rates of both association and dissociation reactions that are markedly reduced. It is thus possible to decouple the qualitative correlation between the binding equilibrium constant and the dissociation rate constants observed for simple intercalators.

The ability to selectively vary substituent size and, thus, intercalation kinetics while maintaining fairly constant binding free energy offers the chance to develop important medicinal agents as well as probes for large-amplitude DNA dynamics (Yen et al., 1982; Sheardy et al., 1989; Wilson et al., 1990c). In their studies of the DNA interactions of a series of actinomycin derivatives, Muller and Crothers (1968) pointed out that medicinal activity was better correlated with binding kinetics than with binding strength. Similar observations have been made with several series of anthracyclines (Wilson et al., 1976; Gabbay et al., 1976), anthraquinones (Krishnamoorthy et al., 1986; Denny & Wakelin, 1990), and acridine analogues of amsacrine (Wakelin et al., 1987, 1990).

Simple hydrodynamic methods can be used to establish intercalation as the binding mode for a compound, but these methods do not resolve classical from threading intercalation modes. These modes can be distinguished by kinetic studies that provide evidence for the different mechanisms characterizing the two binding modes. To define threading intercalation in more details, we present here an investigation of the interaction kinetics of a naphthalene diimide derivative (Figure 1) with DNA. The kinetics of intercalation are analyzed as a function of salt concentration and base pair composition of the DNA and are compared to results for the standard mono- and dicationic phenanthridinium intercalators, ethidium and propidium, to provide a clear distinction between the classical and threading modes (Figure 1). We show that the dependence of the dissociation rate constant on salt concentration is easily measured and provides a sensitive method to distinguish classical intercalation, with both substituents in the same groove, from the threading model in which bulky substituents on the intercalators are in opposite grooves.

Materials and Methods

Synthesis. Naphthalene-1,4,5,8-tetracarboxylic dianhydride (ICN Pharmaceuticals) was purified by refluxing 50 g with 33 g of NaOH and 10 g of charcoal for 2 h, followed by filtration. Acidification of the filtrate yielded golden-brown crystals. The sample was recrystallized from water, washed with ethyl ether, and refluxed with 150 mL of trifluoroacetic acid for 2.5 h. The resulting naphthalene-1,4,5,8-tetracarboxylic acid was refluxed with 600 mL of acetic acid–acetic anhydride (3:1 v/v) for 3 h, filtered, and washed thoroughly with pentane. The dried sample yielded 22 g of beige crystals of naphthalene-1,4,5,8-tetracarboxylic dianhydride. Anal. Calcd for $C_{14}H_4O_6$: C, 62.70, H, 1.50. Found: C, 62.70, H, 1.59.

A 1-g sample of the purified naphthalene-1,4,5,8-tetracarboxylic dianhydride and 10 mL of 2-(dimethylamino)-ethylamine were refluxed in 10 mL of tetrahydrofuran for 8 h. Solvent and excess amine were removed, and the resulting oil was dissolved in 100 mL of dichloromethane and filtered. The organic layer was washed with saturated sodium bicarbonate solution followed by a water wash. The solvent was reduced to 10 mL, and addition of 10 mL of ethanol yielded 1.4 g of yellow crystals. The crystals were dissolved in 15 mL of methanol, and a stream of HBr gas was bubbled into the solution at 0 °C until it was saturated with HBr. A solid precipitated and was recrystallized from water to give 1.6 g of light yellow crystals (mp >300 °C dec). The aromatic NMR spectrum in D_2O has a 12 H methyl singlet at 2.9 ppm, a 4 H triplet at 3.5 ppm, a 4 H triplet at 4.5 ppm, and a 4 H aromatic singlet at 8.6 ppm. Anal. Calcd for $C_{22}H_{26}N_4O_4Br_2$: C, 46.34, H, 4.60, N, 9.82. Found: C, 46.54, H, 4.66, N, 9.80.

Materials. MES buffer contained 1×10^{-2} M 2-(*N*-morpholino)ethanesulfonic acid and 1×10^{-3} M EDTA.[1] Sodium chloride was added to adjust the ionic strength to the desired value, and the pH was adjusted to 6.2. Poly[d(G-C)]$_2$ and poly[d(A-T)]$_2$ were purchased from P-L Biochemicals and

[1] Abbreviations: CT-DNA, calf thymus deoxyribonucleic acid; EDTA, ethylenediaminetetraacetic acid; poly[d(A-T)]$_2$, poly[d(A-T)]·poly[d(A-T)]; poly[d(G-C)]$_2$, poly[d(G-C)]·poly[d(G-C)]; SDS, sodium dodecyl sulfate; NMR, nuclear magnetic resonance.

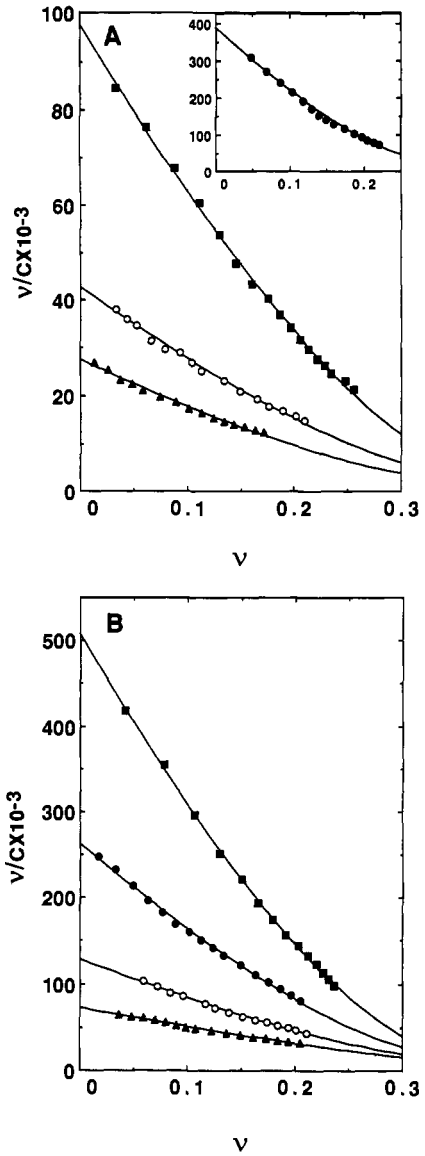

FIGURE 2: Scatchard plots for binding of the naphthalene diimide to (A) poly[d(A-T)]$_2$ and (B) poly[d(G-C)]$_2$. Experiments were at 25 °C in MES buffer at different ionic strengths: (A) (●) 0.05 M NaCl, $K = 3.9 \times 10^5$; (■) 0.10 M NaCl, $K = 9.8 \times 10^4$; (○) 0.15 M NaCl, $K = 4.3 \times 10^4$; and (▲) 0.20 M NaCl, $K = 2.7 \times 10^4$. (B) (■) 0.20 M NaCl, $K = 5.1 \times 10^5$; (●) 0.30 M NaCl, $K = 2.6 \times 10^5$; (○) 0.45 M NaCl, $K = 1.3 \times 10^5$; and (▲) 0.60 M NaCl, $K = 7.2 \times 10^4$. Points in the figure are experimental results, and the solid lines are the best fits from the McGhee–von Hippel site-exclusion model with $n = 2$ and $\omega = 0.9 \pm 0.2$.

prepared as previously described (Wilson et al., 1985b, 1986).

Spectrophotometric Analysis and Binding. Scans, extinction coefficients, and equilibrium constants were determined as previously described (Wilson et al., 1985a; Wilson & Lopp, 1979) with a Cary 2200 spectrophotometer.

Kinetics. Kinetics measurements were conducted with Hi-Tech SF-51 stopped-flow spectrometer. The software provided with the instrument was used for both data acquisition and analysis. Data acquisition was carried out via a high-speed 12-bit analog to digital converter in an HP-330 computer interfaced to the SF-51 stopped-flow spectrometer. Single-wavelength kinetic records of absorbance versus time were collected. Typically, several individual dissociation experiments were collected and averaged by the computer to improve the signal to noise ratio. Dissociation reactions were monitored by mixing equal volumes (100 μL) of polymer–naphthalene diimide complex with a 1% solution of SDS at the same salt concentration. Association kinetics measurements were conducted under pseudo-first-order conditions with excess polymers. Equal volumes (100 μL) of a polymer solution and a solution of naphthalene diimide were mixed. The temperature was controlled by circulating water with a Haake A81 refrigerated water bath and was monitored with an internal thermistor in the SF-51 sample compartment.

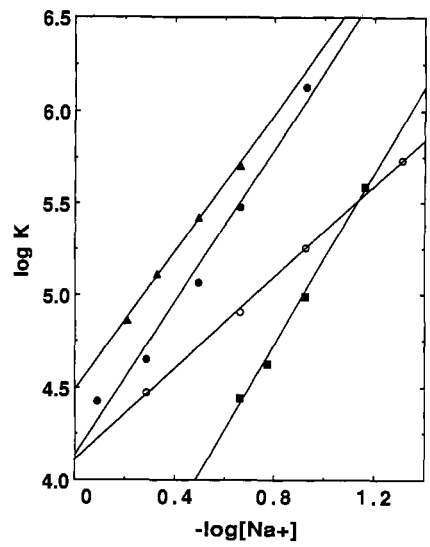

FIGURE 3: Plots of log K, the observed equilibrium constants, determined as in Figure 2, vs −log [Na^+]: naphthalene diimide/poly-[d(A-T)]$_2$ (■), naphthalene diimide/poly[d(G-C)]$_2$ (▲), ethidium/CT-DNA (○), and propidium/CT-DNA (●). The solid lines are linear least-squares best-fit values. Ethidium and propidium have very similar plots for AT and GC polymers as with CT-DNA (Wilson et al., 1985a,b, 1986).

Results

Spectrophotometric Binding Studies. Addition of poly[d-(A-T)]$_2$ and poly[d(G-C)]$_2$ produced similar spectral shifts in the naphthalene diimide absorption spectrum (Figure S1, supplementary material), and the changes are similar to those previously reported for CT-DNA (Yen et al. 1982). Diimide titrations with poly[d(A-T)]$_2$ had isosbestic points at 390 and 302 nm, and with poly[d(G-C)]$_2$, at 390 and 311 nm (Figure S1). The diimide extinction coefficient is 26 600 M^{-1} cm^{-1} at 382 nm, the wavelength maximum for the free compound, and it drops to 10 100 M^{-1} cm^{-1} in the poly[d(A-T)]$_2$ complex and 9800 M^{-1} cm^{-1} in the poly[d(G-C)]$_2$ complex at the same wavelength. With these extinction coefficients at 382 nm, where the optimum changes were obtained, spectrophotometric titration results at several ionic strengths were converted to Scatchard plots for poly[d(A-T)]$_2$ (Figure 2A) and poly[d-(G-C)]$_2$ (Figure 2B). The binding curves with both polymers are well fitted with the site-exclusion model of McGhee and von Hippel (1974). Values for K, n, and ω from the fits in Figure 2 are in the figure legend, and as can be seen, the naphthalene diimide binds significantly more strongly to poly[d(G-C)]$_2$ than to poly[d(A-T)]$_2$. The ω value is the noncooperative value of 1 and n is the neighbor exclusion value of 2, within experimental error, over the entire experimental salt concentration range.

The observed equilibrium constants (K) with both polymers decrease with increasing salt concentration. In Figure 3 log K is plotted as a function of −log [Na^+], and results for the monocationic ethidium and dicationic propidium intercalators are included for comparison (Wilson et al., 1985a). As predicted by the ion condensation theory for polyelectrolytes (Manning, 1978; Record et al., 1978; Wilson et al., 1985a), the slopes for the diimide with AT and GC polymers and for

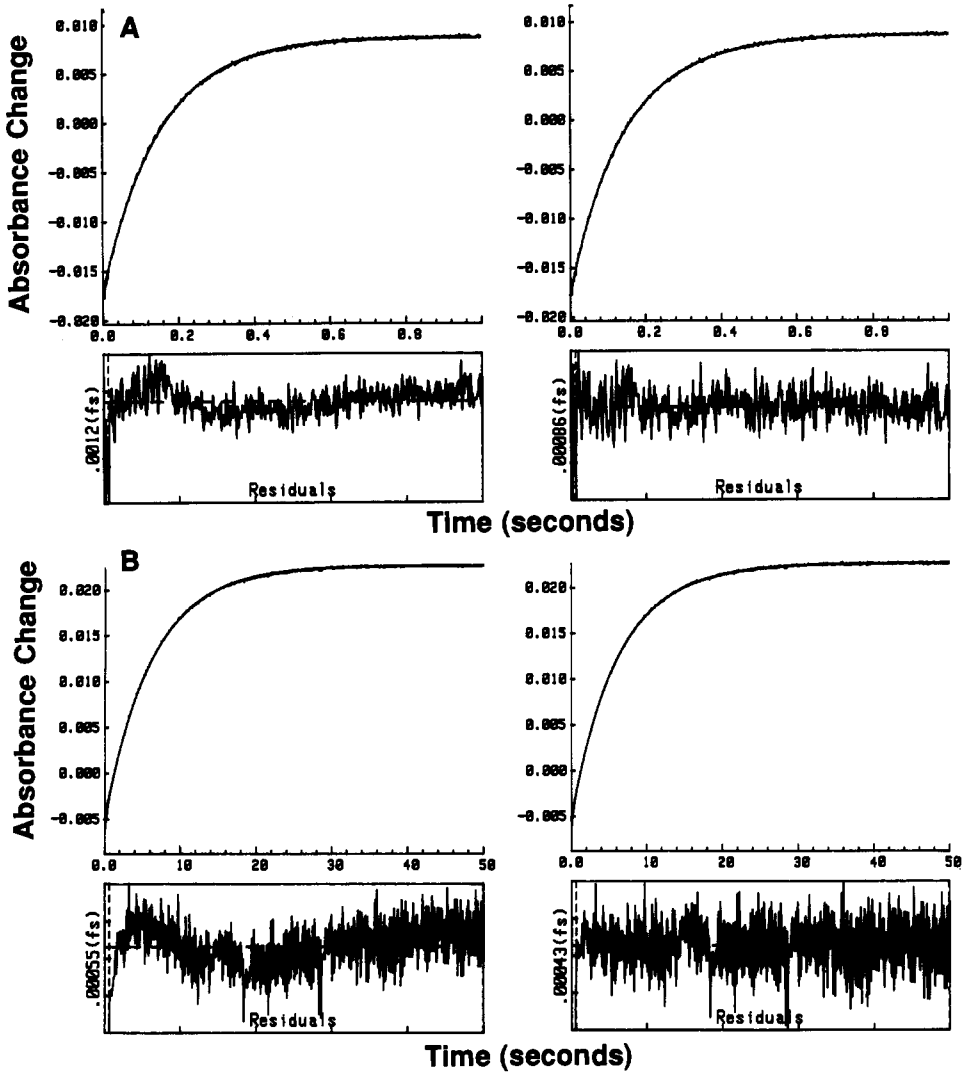

FIGURE 4: Stopped-flow kinetics traces for the SDS-driven dissociation of the naphthalene diimide (A) from poly[d(A-T)]$_2$ at 20 °C and (B) poly[d(G-C)]$_2$ at 25 °C. The experiments were conducted in MES buffer with 0.10 M NaCl at a ratio of 1:10 naphthalene diimide to polymer base pairs. The concentration of the naphthalene diimide after mixing was 6.25×10^{-6} M. The smooth lines in panels A and B are the one-exponential (left side) and two-exponential (right side) fits to the experimental data. Residual plots for both fits are shown under each experimental plot.

propidium are approximately 2 (2.1 ± 0.2). The slope for ethidium is 1.2. The GC binding constants for the diimide are slightly greater than those for propidium, but the AT binding constants are less. The diimide binding to the GC polymer is 20–25 times stronger than to the AT polymer over a range of salt concentrations (Figure 3). Because of its lower slope, the ethidium binding constant is similar to that for the diimide with AT at low salt concentration but is similar to the diimide–GC binding constant at high salt concentration. These results illustrate the problem of comparing DNA binding constants for compounds of different charge under a single set of conditions.

Stopped-Flow Kinetics: Dissociation. Typical stopped-flow kinetics traces for the SDS-driven dissociation of naphthalene diimide from poly[d(A-T)]$_2$ and poly[d(G-C)]$_2$ are shown in Figure 4. Plots are shown for single- and dual-exponential best-fit curves to the data along with plots of residuals. With both polymers there was a significant improvement, based on rms deviation and the distribution of the residuals, in fitting with dual-exponential relative to single-exponential curves under the conditions of these experiments. No significant improvement in rms or residuals is observed on going to a three-exponential fit. The two rate constants for the dual-exponential fits with both polymers differ by less than a factor of 2 (Table I), and such similar processes can only be resolved under the high-resolution stopped-flow conditions illustrated in Figure 4. The dissociation rate increases by over a factor of 50 at the same temperature in going from poly[d(G-C)]$_2$ to poly[d(A-T)]$_2$ (Table I). With both polymers the amplitude for the fast phase of the reaction accounts for 30–40% of the total amplitude under all conditions used.

Table I: Salt Dependence of Naphthalene Diimide Dissociation Rate Constants[a]

[Na$^+$]	k_1 (s^{-1})	$\%A_1$	k_2 (s^{-1})	$\%A_2$	τ (s)
		Poly[d(G-C)]$_2$			
0.135	0.20	43	0.13	57	6.10
0.235	0.28	28	0.16	72	5.25
0.335	0.34	29	0.17	71	4.58
0.485	0.34	31	0.21	69	4.00
0.635	0.39	30	0.23	70	3.57
		Poly[d(A-T)]$_2$			
0.035	7.23	33	3.70	64	0.21
0.055	7.91	36	4.65	64	0.17
0.085	8.99	38	4.97	62	0.15
0.135	10.50	32	5.61	68	0.14
0.235	12.10	30	6.35	70	0.12

[a] All experiments were conducted in MES buffer at 25 °C for the GC polymer and at 20 °C for the AT polymer.

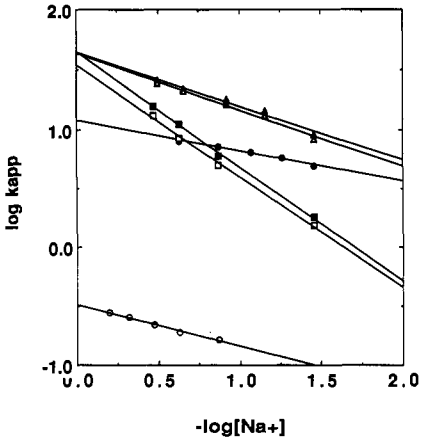

FIGURE 5: Plots of log k_{app} vs −log [Na^+] for dissociation of the naphthalene diimide from poly[d(A-T)]$_2$ (●) and poly[d(G-C)]$_2$ (○); for ethidium from poly[d(A-T)]$_2$ (▲) and poly[d(G-C)]$_2$ (△); and for propidium from poly[d(A-T)]$_2$ (■) and poly[d(G-C)]$_2$ (□). Experiments were conducted in MES buffer at different ionic strengths in the manner described in Figure 4.

The dissociation rate constants for the naphthalene diimide from both polymers were measured at several salt concentrations, and the results are collected in Table I. To simplify comparisons, the dissociation lifetime (τ) and apparent rate constant ($k_{app} = 1/\tau$) were calculated from the computer-derived best-fit values for rate constants and amplitudes as suggested by Denny and Wakelin (1985):

$$\tau = 1/(A_1k_1 + A_2k_2) \quad (1)$$

where A and k values refer to the fractional amplitudes and rate constants for the two exponential fits to the results (Table I). Plots of log k_{app} as a function of −log [Na^+] are shown in Figure 5. The slopes for dissociation of both complexes are 0.30 ± 0.05. Plots of log k_1 and k_2 as a function of −log [Na^+] (Figure S2, supplementary material) are more crowded but give the same slopes, within experimental error, as with k_{app}. For comparative purposes dissociation rate constants for ethidium and propidium are also plotted in Figure 5. With the AT and GC polymers the propidium slopes are 0.7–0.8 and the ethidium slopes are 0.3–0.4. Unlike the diimide, the dissociation rate constants for ethidium and propidium do not vary significantly as the DNA sequences are changed from poly[d(G-C)]$_2$ to poly[d(A-T)]$_2$ or to CT-DNA.

Stopped-Flow Kinetics: Association. The association reactions of the naphthalene diimide with poly[d(G-C)]$_2$ and poly[d(A-T)]$_2$ were measured as a function of DNA concentration at a salt concentration of [Na^+] = 0.2 M and with an approximately 10-fold molar excess of polymer base pairs over the naphthalene diimide. Increasing the ratio to 20 and 30, at constant polymer concentration, had no significant effect on the rate constant, as expected for a pseudo-first-order reaction. A typical association kinetics plot for the naphthalene diimide complex with poly[d(G-C)]$_2$ is shown in Figure 6. As with dissociation experiments, satisfactory fits were not obtained with single but were obtained with dual-exponential curves (Figure 6). The differences in the rate constants for the two exponential fits were 2–3, and k_a^{app} values were calculated with eq 1.

Apparent association rate constants determined at several concentrations of poly[d(G-C)]$_2$ and poly[d(A-T)]$_2$ fit the relation:

$$k_a^{app} = k_a[DNA] + k_d \quad (2)$$

where [DNA] is the molar concentration of polymer in base pairs, k_a^{app} is the pseudo-first-order apparent association rate constant at each polymer concentration, and k_a is the intrinsic second-order association rate constant. The plot is linear within experimental error (Figure S3), and the slope of the line gives the second-order association rate constant, while the intercept gives the calculated dissociation rate constant for these conditions (Table II and Figure S3, supplementary material). The measured dissociation rate constant for the naphthalene diimide from poly[d(G-C)]$_2$, 0.20 s^{-1} at 25 °C in 0.24 M [Na^+], is in good agreement with the k_d value from eq 2, 0.21 s^{-1}. The measured dissociation rate constant for naphthalene diimide from poly[d(A-T)]$_2$, 8.1 s^{-1} at 20 °C in 0.24 M [Na^+], is also in good agreement with the k_d value from eq 2, 7.4 s^{-1}. We have previously found that the observed pseudo-first-order association rate constants for ethidium and propidium are also linear in DNA concentration (Wilson et al., 1985a,b, 1986).

Discussion

Hydrodynamic and spectroscopic studies have shown that naphthalene diimides bind to DNA by intercalation (Yen et al., 1982). Many heterocyclic and/or highly polarizable in-

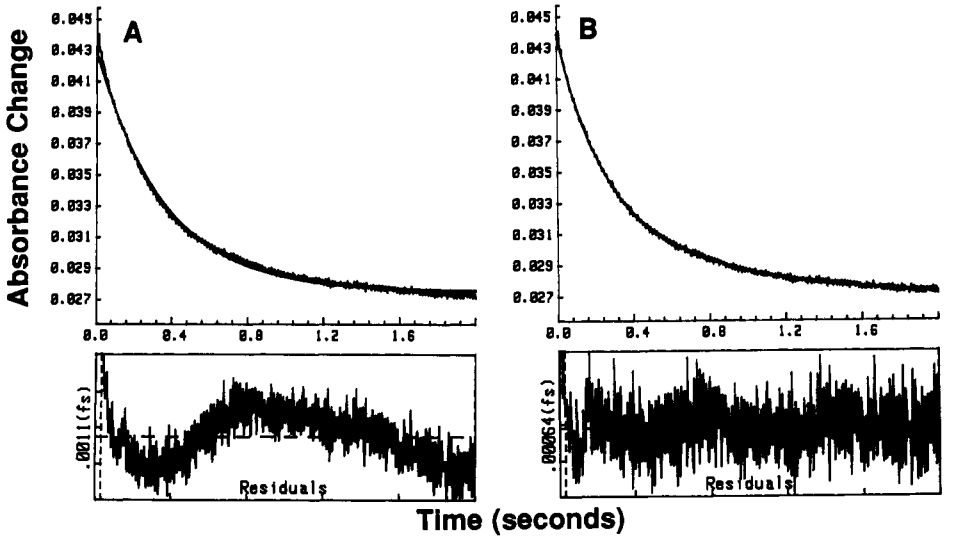

FIGURE 6: A stopped-flow kinetics association reaction for the naphthalene diimide with poly[d(G-C)]$_2$. The total concentrations after mixing were 2.5 × 10^{-5} M for polymer (base pairs) and 2.5 × 10^{-6} M for the naphthalene diimide in MES buffer with 0.20 M added NaCl at 25 °C for poly[d(G-C)]$_2$. The smooth lines in panels A and B are the one- and two-exponential fits to the experimental data, respectively. Residual plots for both fits are shown under each experimental plot.

tercalators exhibit a binding preference for GC base pairs with the larger asymmetric charge distribution (larger dipole moment) of GC relative to AT base pairs (Saenger, 1984) probably accounting for a significant portion of the GC specificity (Muller & Crothers, 1975). Although the naphthalene diimides that we have synthesized are symmetric, they still have significant partial atomic charges on the heterocyclic rings, and the molecule in Figure 1, for example, exhibits significant GC binding specificity. As can be seen in Figure 3, the diimide binding constant to poly[d(G-C)]$_2$ is approximately 20–25 times larger than for poly[d(A-T)]$_2$ over a range of salt concentrations. Similar plots for the strong binding mono- and dicationic phenanthridinium intercalators, ethidium and propidium (Figure 3), illustrate that on a relative scale the interactions of the naphthalene diimide with DNA are quite favorable. The GC interactions are particularly strong, and the AT binding is only slightly less than for ethidium and propidium.

The counterion condensation theory predicts that the slopes of log K versus log [Na^+] plots in Figure 3 should be approximately equal to the number of ion pairs the ligands form in their DNA complexes (Record et al., 1978; Wilson et al., 1985a; Lohman et al., 1985). Thus, the monocationic ethidium has slope near 1 while dicationic propidium and naphthalene diimide have slopes near 2 (Wilson et al., 1985a; Wilson & Lopp, 1979). At [Na^+] = 1 M, the calculated thermodynamic binding constants are $\sim 10^3$ M^{-1} for the diimide with AT and $>10^4$ M^{-1} for propidium and ethidium with DNA and for the diimide with GC. These values represent the intrinsic binding affinities of the ligands with DNA (e.g., contributions from van der Waals, hydrogen bonding, electrostatic, hydrophobic interactions) (Record et al., 1978).

At lower salt concentrations the binding becomes more favorable due to the favorable entropy of counterion release from DNA on binding of the cationic ligands. We have found that quite diverse heterocyclic intercalators have thermodynamic binding constants ([Na^+] = 1 M) near 10^3 M^{-1} (Wilson & Lopp, 1979; Fairley et al., 1988; unpublished results) as the diimide has with AT base pairs. The intrinsic interactions of propidium and ethidium with DNA and the diimide GC are, thus, significantly more favorable than this typical value. With ethidium and propidium at least part of the additional favorable binding energy probably comes from favorable electrostatic and hydrogen-bonding interactions of the amino substituents with DNA phosphate groups at the intercalation site (Jain et al., 1977; Tsai et al., 1977). These interactions depend more on DNA conformation than on base pair type, and ethidium and propidium, thus, do not show large base pair binding specificity. With the diimide, the larger ring system provides favorable van der Waals stacking interactions and the partial atomic charges on the heterocyclic rings can provide favorable Coulombic interactions, particularly with GC base pairs.

Two quite different types of intercalation complexes of the naphthalene diimide with DNA are possible. In one complex the edge of the naphthalene diimide ring systems stacks with base pairs in a partial intercalation complex and both cationic substituents bind in the same groove. In the second type of complex, a threading binding mode, one side chain of the naphthalene diimide is in each of the DNA grooves and the aromatic ring system forms strong stacking interactions with the DNA base pairs. The large increases in linear DNA viscosity (Yen et al., 1982), large diimide hypochromicity on binding to DNA (Figure S1), large upfield shifts of the diimide aromatic protons signals on binding to DNA (not shown), and the strong DNA interactions of the naphthalene diimide indicate that it binds to DNA by the threading mechanism. In the threading model passing the side chain between base pairs during intercalation should significantly slow both association and dissociation reactions, and kinetics studies, thus, offer a straightforward method for distinguishing between threading and nonthreading intercalation binding modes.

Table II: Comparison of Binding Constants Calculated from Kinetic Rate Constants and Determined from Equilibrium Binding Experiments[a]

complex	k_a ($\times 10^{-5}$) (M^{-1} s^{-1})[b]	k_d (s^{-1})[b]	log K kinetics[c]	log K equilibrium
naphthalene diimide/poly[d(G-C)]$_2$	1.4	0.21	5.6	5.7
naphthalene diimide/poly[d(A-T)]$_2$	3.4	7.4	4.7	4.4
propidium/CT-DNA[d]	10.6	6.7	5.2	5.5

[a] All experiments were conducted in MES buffer with 0.2 M added NaCl at 25 °C for the GC polymer and at 20 °C for the AT polymer. [b] k_a and k_d values are from the slope and intercept from eq 2 and Figure S3, supplementary material. [c] Calculated from the ratio of k_a/k_d. [d] Data from Wilson et al. (1985a); at 15 °C.

The naphthalene diimide dissociation rate constants are compared to those for propidium and ethidium at a range of salt concentrations in Figure 5, and both dissociation and association results are compared in Table II. Several key features emerge from these comparisons. First, the propidium second-order association rate constant is approximately 5 times larger than that for the AT and 10 times larger than for the GC association constant of the naphthalene diimide. Second, even though propidium binds significantly more strongly to DNA than the naphthalene diimide to AT sequences (Figure 3), the two compounds have similar dissociation rate constants (Table II). Propidium and the naphthalene diimide with GC sequences have similar binding equilibrium constants, but the propidium dissociation rate constant is approximately 50 times larger than for the naphthalene diimide dissociation from GC sites at the same temperature. Clearly, under comparable binding conditions, the naphthalene diimide associates and dissociates from DNA much more slowly than propidium, which is structurally constrained to have its bulky substituents and both of its charges in the same DNA groove (Figure 1). Naphthalene monoimides (Yen et al., 1982), which have only one imide side chain, associate and dissociate from DNA so rapidly that their kinetics are outside of the stopped-flow range. These observations strongly support the threading model for the diimide intercalation complex and illustrate that side chains of rather modest size can have large effects on DNA interaction kinetics.

In addition to the absolute rates, the slopes are a particularly important feature of the plots in Figure 5. The counterion condensation theory and experimental observations indicate that classical monocationic intercalators should have slopes of 0.3–0.4 and dicationic intercalators slopes of 0.6–0.8 in such plots (Wilson et al., 1985a). Dicationic groove binding ligands, by comparison, have slopes in log k_d versus −log [Na^+] plots of 1.6–1.8 (Wilson et al., 1989a, 1990a–c). Dissociation kinetic rate constants as a function of salt concentration can generally be determined quite accurately, and the log k_d versus −log [Na^+] plots are, thus, an excellent experimental method for determining the binding mode of charged ligands with different DNA sequences (Lohman et al., 1978, Lohman, 1985; Wilson et al., 1985a, 1989a, 1990a–c).

As can be seen in Figure 5, however, the diimide slopes do not fit the predicted values for a dication binding to DNA as a classical intercalator or as a groove binding agent. The

diimide slopes in Figure 5 are close to those predicted for a classical intercalator with a single charge. These results, however, can be explained by the threading mechanism for a dicationic intercalator. The rate-determining step in dissociation of a dicationic threading intercalator is release of one side chain interaction followed by the free side chain sliding between base pairs to the opposite DNA groove. Complete dissociation of the compound can then occur in a fast reaction step in the overall dissociation mechanism. Thus, even though the diimide forms two ion pairs in its DNA complex (Figure 3), the rate-determining step in the dissociation involves release of only one of these ion pairs and the log k_d versus $-\log [Na^+]$ slope is similar to that observed for simple monocationic intercalators. These kinetics studies, thus, distinguish cationic intercalators that bind by the classical intercalation mechanism from those that bind by the threading mechanism, and they provide additional evidence that the naphthalene diimide of Figure 1 binds to DNA in a threading complex. Kinetics studies have also proven crucial in establishing the binding modes of a series of diphenylfuran derivatives that bind to DNA by groove, classical, and threading interaction modes (Wilson, 1990c).

Supplementary Material Available

Spectral shifts of the naphthalene diimide on titration with poly[d(A-T)]$_2$ and poly[d(G-C)]$_2$ (Figure S1), plots of log k_1 and log k_2 versus $-\log [Na^+]$ for dissociation of the naphthalene diimide from poly[d(A-T)]$_2$ and poly[d(G-C)]$_2$ (Figure S2), and plots of k_a^{app} as function of polymer concentrations in base pairs with poly[d(A-T)]$_2$ and poly[d(G-C)]$_2$ (Figure S3) (4 pages). Ordering information is given on any current masthead page.

Registry No. Poly[d(A-T)]$_2$, 26966-61-0; poly[d(G-C)]$_2$, 36786-90-0; naphthalene-1,4,5,8-tetracarboxylic dianydride, 81-30-1; 2-(dimethylamino)ethylamine, 108-00-9; naphthalene diimide, 81254-00-4.

References

Abraham, Z. H. L., Agbandje, M., Neidle, S., & Acheson, R. M. (1988) *J. Biomol. Struct. Dyn. 6*, 471–488.

Delbarre, A., Delepierre, M., Langlois D'Estaintot, M., Igolen, J., & Rogues, B. P. (1987) *Biopolymers 26*, 1001–1033.

Denny, W. A., & Wakelin, L. P. G. (1990) *Anti-Cancer Drug Des. 5*, 189–200.

Denny, W. A., Baguley, B. C., & Cain, B. F. (1983) in *Molecular Aspects of Anticancer Drug Action* (Neidle, S., & Waring, M. J., Eds.) MacMillan Press, London.

Denny, W. A., Atwell, G. J., Baguley, B. C., & Wakelin, L. P. G. (1985) *J. Med. Chem. 28*, 1568–1574.

Fairley, T., Molock, F., Boykin, D. W., & Wilson, W. D. (1988) *Biopolymers 27*, 1433–1447.

Gabbay, E. J., Grier, D., Fingerle, R. E., Reimer, R., Levy, R., Pearce, S. W., & Wilson, W. D. (1976) *Biochemistry 15*, 2062–2070.

Jain, S. C., Tsai, C. C., & Sobell, H. M. (1977) *J. Mol. Biol. 114*, 317–331.

Krishnamoothy, C. R., Yen, S. F., Smith, J. C., Lown, J. W., & Wilson, W. D. (1986) *Biochemistry 25*, 5933–5940.

Lohman, T. M. (1985) *CRC Crit. Rev. Biochem. 19*, 191–235.

Lohman, T. M., DeHaseth, P. I., & Record, M. T. (1978) *Biophys. Chem. 8*, 281–294.

Manning, G. S. (1978) *Q. Rev. Biophys. 11*, 179–246.

McGhee, J. D., & von Hippel, P. H. (1974) *J. Mol. Biol. 86*, 469–489.

Muller, W., & Crothers, D. M. (1968) *J. Mol. Biol. 35*, 251–290.

Muller, W., & Crothers, D. M. (1975) *Eur. J. Biochem. 54*, 267–277.

Neidle, S., & Abraham, Z. (1984) *CRC Crit. Rev. Biochem. 17*, 73–121.

Record, M. T., Jr., Anderson, C. F., & Lohman, T. M. (1978) *Q. Rev. Biophys. 11*, 103–178.

Record, M. T., Jr., Mazur, S. J., Melanoon, P., Roe, J. H., Shaner, S. L., & Unger, L. (1981) *Annu. Rev. Biochem. 50*, 997–1024.

Saenger, W. (1984) in *Principles of Nucleic Acid Structure*, Springer-Verlag, New York.

Scott, E. V., Zon, G., Marzilli, L. G., & Wilson, W. D. (1988) *Biochemistry 27*, 7940–7950.

Sheardy, R. D., Wilson, W. D., & King, D. H. (1989) in *Chemistry & Physics of DNA–Ligand Interactions* (Kallenbach, N. R., Ed.) pp 175–211, Adenine Press.

Sobell, H. M., & Jain, S. C. (1972) *J. Mol. Biol. 68*, 21–43.

Tsai, C. C., Jain, S. C., & Sobell, H. M. (1977) *J. Mol. Biol. 114*, 301–315.

Wakelin, L. P. G., Atwell, G. J., Rewcastle, G. W., & Denny, W. A. (1987) *J. Med. Chem. 30*, 855–861.

Wakelin, L. P. G., Chetcuti, P., & Denny, W. A. (1990) *J. Med. Chem. 33*, 2039–2044.

Wang, A. H.-J., Ughtto, G., Quigley, G. J., & Rich, A. (1987) *Biochemistry 26*, 1152–1163.

Waring, M. J. (1981) in *The Molecular Basis of Antibiotic Action* (Gale, E. F., Cundiffe, E., Reynolds, P. E., Richmond, M. H., & Waring, M. J., Eds.) 2nd ed., p 287, Wiley, New York.

Wilson, W. D. (1990) in *Nucleic Acids in Chemistry and Biology* (Blackburn, M., & Gait, M., Eds.) Chapter 8, Oxford–IRL Press Ltd., Oxford.

Wilson, W. D., & Lopp, I. G. (1979) *Biopolymers 18*, 3025–3041.

Wilson, W. D., Grier, D., Reimer, R., Bauman, J. D., Preston, J. F., & Gabbay, E. J. (1976) *J. Med. Chem. 19*, 381–384.

Wilson, W. D., Krishnamoorthy, C. R., Wang, Y. H., & Smith, J. C. (1985a) *Biopolymers 24*, 1941–1961.

Wilson, W. D., Wang, Y. H., Krishnamoorthy, C. R., & Smith, J. C. (1985b) *Biochemistry 24*, 3991–3999.

Wilson, W. D., Wang, Y. H., Krishnamoorthy, C. R., & Smith, J. C. (1986) *Chem.-Biol. Interact. 58*, 41–57.

Wilson, W. D., Strekowski, L., Tanious, F., Watson, R., Mokrosz, J. L., Strekowska, A., Webster, G., & Neidle, S. (1988) *J. Am. Chem. Soc. 110*, 8292–8299.

Wilson, W. D., Tanious, F. A., Barton, H. J., Strekowski, L., Boykin, D. W. & Jones, R. L. (1989a) *J. Am. Chem. Soc. 111*, 5008–5010.

Wilson, W. D., Tanious, F. A., Watson, R. A., Barton, H. J., Strekowska, A., Harden, D. A., & Strekowski, L. (1989b) *Biochemistry 28*, 1984–1992.

Wilson, W. D., Tanious, F. A., Barton, H. J., Jones, R. L., Fox, K., Wydra, R. L., & Strekowski, L. (1990a) *Biochemistry 29*, 8452–8461.

Wilson, W. D., Tanious, F. A., Barton, H. J., Wydra, R. L., Jones, R. L., Boykin, D. W., & Strekowski, L. (1990b) *Anti-Cancer Drug Des. 5*, 31–42.

Wilson, W. D., Tanious, F. A., Buczak, H., Venkatramanan, M. K., Das, B. P., & Boykin, D. W. (1990c) in *Jerusalem Symposia on Quantum Chemistry and Biochemistry: Molecular Basis of Specificity in Nucleic Acid–Drug Interactions* (Pullman, B., & Jortner, J., Eds.) Vol. 23, pp 331–352, Kluwer Academic Publishers, Amsterdam.

Yen, S. F., Gabbay, E. J., & Wilson, W. D. (1982) *Biochemistry 21*, 2070–2076.